Incident laser modulation by tool marks on micro-milled KDP crystal surface: Numerical simulation and experimental verification

Qi Liu[1,3,4], Jian Cheng[1,2,4,*], Zhirong Liao[3], Hao Yang[2], Linjie Zhao[2], Mingjun Chen[1,2,*]

[1]State Key Laboratory of Robotics and System, Harbin Institute of Technology, Harbin 150001, China
[2]Center for Precision Engineering, Harbin Institute of Technology, Harbin 150001, China
[3]Machining and Condition Monitoring Group, Faculty of Engineering, University of Nottingham, NG7 2RD, UK
[4]These authors contributed equally to this work

Corresponding author:

P.O. Box 413, Harbin 150001， P.R. China

Tel.: +86(0)451-86403252

Fax: +86(0)451-86403252

Email: chenmj@hit.edu.cn and cheng.826@hit.edu.cn

Abstract

Micro-milling has been accepted as the most promising method to repair the micro-defects on the surface of KH_2PO_4 (KDP) optics. However, surface tool marks are inevitably introduced during the micro-milling repairing process, and could possess great potential risks in lowering the laser-induced damage threshold of KDP optics. The primary cause of laser damage growth of nonlinear crystals has been considered as its internal light intensification. In this work, how the tool marks impact the incident laser modulation as well as the laser-induced damage resistance of micro-milled KDP optics was theoretically and experimentally investigated. The results indicate that periodic tool marks can cause diffraction effect and result in significant relative light intensity modulation (I_{Rmax}), up to 5.6 times higher than that inside smooth crystal surfaces. Although the change trends of I_{Rmax} with respect to tool marks on both surfaces of KDP optics are similar, the I_{Rmax} induced by the rear-surface tool marks is nearly twice higher than that induced by the front-surface tool marks, which means the rear surface with tool marks are more vulnerable to be damaged. The period of tool marks determines the modulation degree and distribution patterns of light intensity inside KDP crystal while the residual height of tool marks can only slightly regulate the modulation degree of light intensity. The tool marks with a period of 1 μm normally give rise to serious light intensification and should be strictly excluded, while the period of tool marks from 10 μm to 20 μm is conducive to the laser damage resistance of micro-milled KDP optics, which were verified by the tests of transmittance capacity and laser damage resistance, and is supposed to be preferred in the actual repairing process of full-aperture KDP optics.

Keywords: KDP crystal, laser damage, light intensity modulation, micro ball-end milling, tool marks, surface topography

1. Introduction

As an excellent nonlinear material, potassium dihydrogen phosphate (KH_2PO_4 /KDP) crystals can offer such an excellent combination of large nonlinear optical coefficient with wide transmission spectrum and high intrinsic laser-induced damage threshold (LIDT) [1, 2] that they have been widely applied in the Inertial Confinement Fusion (ICF) projects, such as the National Ignition Facility (NIF) in USA [3], the LMJ facility in France [4] and the SG-III in China [5]. Nevertheless, owing to its weak mechanical properties (soft and brittle), KDP optical component has been regarded as one of the most difficult-to-fabricate materials among the optics required by the ICF laser facilities. And it is extremely vulnerable to introduce some micro-defects (e.g., cracks, pits, ablation) on the surface of KDP optics during both the diamond ultra-precision machining and laser pre-irradiating processes [6]. Once these micro-defects occur on the optical surface, they would dramatically grow under the subsequent high-power laser irradiation and eventually cause the whole optical elements to be scrapped. Considering the time-consuming and costly process of crystal growth, the most economical way is to repair the optical component by replacing those original defects with predesigned smooth contours, which is termed as “optical recycle loop strategy” that firstly proposed by Lawrence Livermore National Laboratory (LLNL) [7].

To achieve the “loop strategy”, considerable efforts have been devoted to exploring the effective techniques to mitigate the surface defects on optics during the last decades [8-11]. Some advanced approaches, including CO_2 laser melting, water etching and short-pulse laser ablation as well as micro machining, have been utilized to repair the micro-defects on the KDP surface. After comparing the outcomes of above methods, it is accepted that micro-milling is the most promising method to complete repair work and can be applied in the future engineering mitigation of laser damage growth on large-aperture KDP optics [10,12]. Nevertheless, it is not a simple and readily available task to remove micro-defects effectively and then curb the damage growth of KDP optics because there are many factors having great influences on the repairing results, including the targeted design of repair contours [13,14], the ductile-regime cutting of KDP brittle crystal [15-17], the optimization of process parameters [18,19], etc.

In recent years, research interest on the micro-milling of micro-defects on optical surface has mainly divided into two respects. One is to investigate how to design suitable repair contours for different types of defects on the promise of ensuring the minimum material removal [13,14]. For instance, the centrosymmetric contours like Gaussian contours are supposed to take place of the defect sites with circle shapes like homogeneously melted damage, while the elongated contours like Ellipsoidal contours ought to replace the defect sites with large length-width ratios like radial cracks and surface scratches [20]. Even with the same kind of contours, different width-to-depth ratios have distinct influences on the internal light intensification and LIDT of crystal optics [13]. The other one is to probe into the machining mechanism to achieve a fracture-free surface on KDP crystal through micro-milling method [17,18]. Due to the soft-brittle properties, brittle fracture can be easily generated on the crystal surface by even very small cutting forces, resulting in the formation of surface and subsurface damage [21]. The investigations on brittle-to-ductile transition [15,16] and ploughing effect [22] are an effective preliminary to ensure that the machining process is performed in ductile-regime and a smooth machined surface could be achieved. However, to the best of our knowledge, little attention has been paid on the topography of repaired surface and its real influence on the laser-induced damage resistance of KDP optics. Hence, a great effort is supposed to be made to investigate how the surface topography of repaired KDP optics affects the optical performance.

At present, most research work about surface topography is focused on the relationships between the feature structures on surface and their scattering performance and focusing coupling effect [23-26]. But little work has been reported to investigate the influence of machined surface topography on the optical performance of optics under the environment of high laser irradiation. In actual repairing process, a micro ball-end milling cutter is used to sweep the micrometer-sized defects or damaged sites away along a given machining paths, and convert them into predesigned contours which are normally about 1mm width and tens of micrometers depth in size [14]. When the cutter moves along adjacent paths, periodic tool marks are unavoidable to be left on the machined surface owing to the spherical geometry of the cutter [27]. The tool marks possess two characterize parameters: residual height (*H*) and period (*P*) which are normally less than 30 μm, jointly determining the topography of the machined surface. These micro-milled tool marks are quietly different from micro-waves generated in single point diamond fly cutting process which is normally used for fabricating KDP bulk material (410mm×410mm) [28, 29]. The micro-waves are normally represented by characteristic frequency, and the most dangerous micro-waves (200^{-1} μm^{-1} to 90^{-1} μm^{-1}) for laser damage are found to be closely related to the spindle vibration of fly-cutting system [30]. Meanwhile, Li [29] reported that the tool marks generated in fly cutting process are very slight and their impacts on LIDT can be ignored. However, the dimension of micro-milled tool marks is so close to incident wavelength that these tool marks can not be neglected [31]. Therefore, the generation mechanism and characteristic parameters between micro-milled tool marks and micro-waves are completely different from each other, indicating distinct impacts on the optical performance of KDP optics.

In fact, the laser irradiation process for micro-milled KDP crystal can be considered as the propagation of an electromagnetic wave through whole KDP optics, which conforms to the theory of wave optics. Thus, all optical phenomena (including but not limited to light intensification, diffraction effect, scattering effect and interference effect) could have different impacts on the eventual incident laser modulation. But the influencing extent of each factor depends on the structure features of the irradiated items. For example, the scattering effect could play a dominant role in the light field modulation when laser irradiates on nanoscale impurity particles adhered on optic surfaces [32].

While for repaired KDP optics processed by micro-milling, the period of residual tool marks is usually dozens of micrometers while the corresponding residual height is several hundreds of nanometers. These tool marks dimensions are so close to the laser working wavelength in ICF facilities that severe diffraction effect could be brought about inside the repaired optics and result in significant light intensity modulation [28,33]. And the light intensification has been widely regarded as the primary cause of the laser damage growth of nonlinear crystals in ICF facilities [34]. But to the best of authors' knowledge, no work has been reported to reveal the theoretical relationship between the residual tool marks and their induced light intensification inside repaired KDP optics. Therefore, the evaluation of micro-milled KDP surface and its light performance are in urgent need of systematical investigations to provide guidelines for the optimization of its micro-milling process and the future engineering repair of full-aperture KDP components.

To address the research gaps mentioned above, this paper aims to explore the effect of tool marks on the incident laser modulation. The morphologies of tool marks on micro-milled KDP surfaces were firstly characterized via white light interference (WLI). Then, on the basis of the tested characteristic parameters, finite element method (FEM) models were established to simulate the light intensity modulation induced by tool marks inside micro-milled KDP crystal. The influence of period and residual height of tool marks on the modulation property to incident lasers was theoretically investigated. At last, the laser damage tests were conducted to verify the theoretical results. This work could be beneficial to the recycling of expensive large-aperture KDP crystal components in ICF facilities and might be an interesting start for further research in the interaction between the surface topography of optics and high power lasers.

2. Material and Experiments

2.1 Fabrication of micro-milled surfaces on KDP crystal

In order to evaluate the influence of tool marks on the incident laser modulation as well as the LIDT of KDP optics, the micro-milled surfaces on KDP crystal were firstly fabricated. Figure 1 displays the machining set-up and the micro ball-end milling cutter used in this work. A rectangular bulk KDP crystal was employed as the specimen, which was processed by single point diamond turning and possessed a nanoscale surface roughness. As shown in Fig. 1(a), a miniature fix-axis vertical spindle machine tool was utilized to perform the micro-milling experiments. It can achieve a high rotational speed up to 80, 000 RPM, and more information about this machine tool can be found in [35]. Fig. 1(b) shows the micro ball-end milling cutter with a diameter of 0.5mm. This tool is made of cubic boron nitride (CBN) and has two cutting edges.

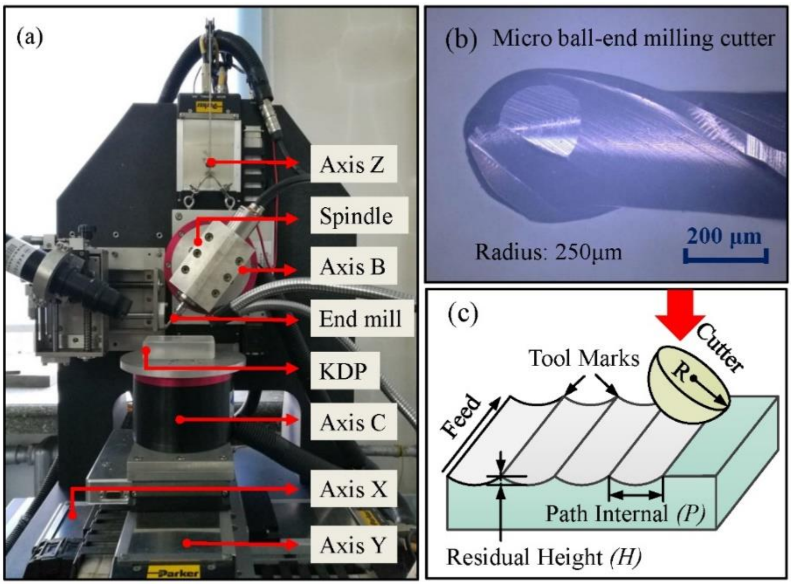

Fig. 1. Pictures of the machining set-up used in this work. (a) The micro-milling five-axis machine tool. (b) The micro ball-end milling cutter. (c) Schematic of the formation of tool marks.

Figure. 1(c) shows the schematic diagram of residual tool marks generated in the micro ball-end milling process. The micro ball-end milling cutter normally moves along successive cutting paths which are separated by an offset distance (namely path interval). These cutting paths are normally parallel to each other and perpendicular to the feed direction of micro cutter. Meanwhile, the milling cutter also rotates around its axis when it moves along feed direction. Thus, periodical tool marks along both pick direction and feed direction will be generated on the machined surface because of the geometric shape and dynamic movement of the cutter. Two important parameters are generally utilized to describe the characteristics of tool marks. One is the period, indicating the path interval (P) of successive cutting paths; the other one is the residual height (H), illustrating the height of path-interval scallop which is generated between adjacent tool paths. But it is noteworthy that in manufacturing of KDP brittle crystal, the employed feed per tooth (less than 0.5 μm) is very small to obtain a smooth and fracture-free surface. This leads to very small tool marks along feed direction, which can only cause slightly evanescent waves, and their influence on the laser damage resistance of KDP optics can be ignored [29]. Therefore, in this work, only the residual tool marks along pick direction was discussed and investigated.

The machining parameters are presented in Table 1. The spindle rotation speed, feedrate and depth of cut were set as 50, 000 RPM, 48 mm/min and 5 μm, respectively. These machining parameters can guarantee the micro-milling process of KDP brittle crystal in ductile regime [17,18]. At the same time, the path intervals of 1 μm, 5 μm, 10 μm, 20 μm and 30 μm were chosen in the micro-milling experiments to fabricate tool marks at different scales, and the optical performance of these tool marks will be evaluated in the following sections.

Table 1. Parameters applied in micro-milling to produce tool marks on KDP surfaces

Cutting tool	Machining process			Machining set-up	
Radius R (μm)	Feed rate f (mm/min)	Cutting depth a_p (μm)	Spindle speed n (RPM)	Lead angle (°)	Spindle inclining angle (°)
250	48	5	5×10^4	+45	45

2.2 Characterization of tool marks on micro ball-end milled KDP surfaces

The machined samples were then detected to acquire the characteristic parameters of tool marks through a white light interferometer (WLI, Newview 8200, Zygo). Figure 2 displays the surface morphology of KDP crystal processed with a path interval of 20 μm. It is found that periodic tool marks along pick direction were produced on the machined surface. The spacing between adjacent tool marks is nearly equivalent to the path interval (P=20 μm) used in the experiment, while the residual height of these tool marks (PV) is nearly 200 nm. This result effectively validates the rightness of above demonstration about the formation mechanism of tool marks. Meanwhile, it is necessary to note that the path interval chosen in practical repair process is generally less than 30 μm for the sake of a smooth surface and lower surface roughness (Ra), and the corresponding residual height are usually in the range from 50 nm to 250 nm based on the topographic observation.

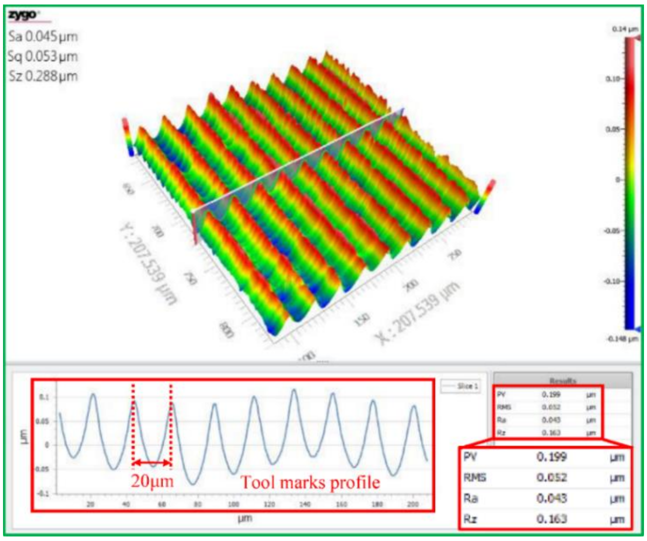

Fig. 2. Morphology of tool marks measured by white light interferometer. The residual height and path interval of tool marks are about 199 nm and 20 μm, respectively.

2.3 Test of the optical performance of micro-milled KDP optics

The tangible impact of various tool marks on the incident laser modulation can be evaluated by the optical transmittance capacity and laser damage resistance of micro-milled KDP optics through laser irradiation experiments. Firstly, the tool marks with periods of 1μm, 10μm, 20μm and 30μm were generated on the sample surfaces according to the milling parameters listed in Table 1. Then, the optical transmittance of these sample surfaces was tested using Lambda 950 spectrophotometer [36], which can measure the transmittance of optics at wavelength from 900 nm to 1200 nm. This instrument possesses a precision measurement resolution up to 0.2 nm with a wavelength of 0.3 nm. Because 1064 nm wavelength is the working wavelength for optical switch KDP crystal applied in ICF facilities, the transmittance at 1064 nm wavelength was picked out after laser irradiation, and was calculated as the average value of 10 sites to qualitatively validate the modulation effect induced by various tool marks.

The laser damage test of micro-milled KDP surfaces with various tool marks was also performed to measure the corresponding LIDTs and further validate their laser damage resistance with respected to the dimensions of tool marks. Figure 3 shows the light path schematic of laser system, which consists of the Nd:YAG lasers, laser focusing lens and high precision translation stage, etc. The intense pulsed lasers used in experiments worked at the wavelength 1064 nm, the pulse duration 10 ns and the pulse repetition frequency 1 Hz [11]. The laser vertically irradiated on micro-milled KDP crystal surface, which was mounted on the 3-axis transition stage. In addition, a charge-coupled device (CCD) was integrated into the measuring system to monitor any damage on the sample surface. The R-on-1 [10,37] laser damage test mode was adopted in the experiment, and for each kind of micro-milled KDP surface, a total of 10 test sites were irradiated with laser fluence ramping up (1 J/cm^2) until the damage takes place. The LIDT is the average value of the lowest fluence corresponding to the initiation of laser damage. The laser fluence was adjusted by the combined action of a polarizer and half-wave plate in laser damage tests. The focal distance of the focusing lens used in this work was 2 m and the equivalent laser spot size was 280 μm. More experimental details on the employed instruments and the used parameters can be found in Refs [11,14].

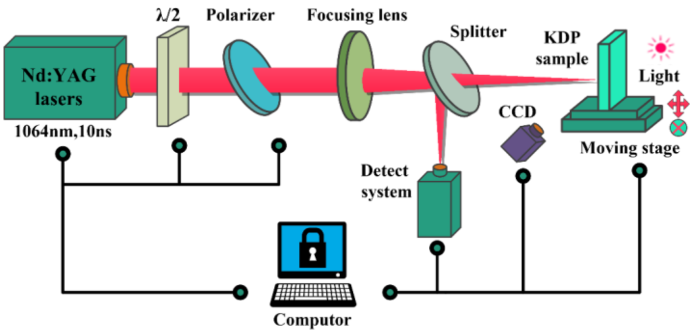

Fig. 3. Schematic of the laser system designed to test the LIDTs of micro-milled KDP surfaces.

3 Theory and simulation calculation

Because the essence of light is an electromagnetic wave, the process of laser irradiation can be considered as the propagation of an electromagnetic wave through micro-milled KDP optics, which conforms to theory of wave optics. On the basis of the rigorous electromagnetic field theory, the finite element method (FEM) is utilized to solve the Maxwell equation and calculate the electric field intensity distribution induced by a series of tool marks with different combination of various periods and residual heights. Since defects usually occur not only on the laser-coming surface (front surface) but also on the laser-outgoing surface (rear surface), the micro-milled tool marks can also appear on the both surfaces of KDP optics in practical ICF facilities. The difference between the effect of front-and rear-surface tool marks on the light field modulation inside KDP crystal is another important content in this work, which will be further discussed below.

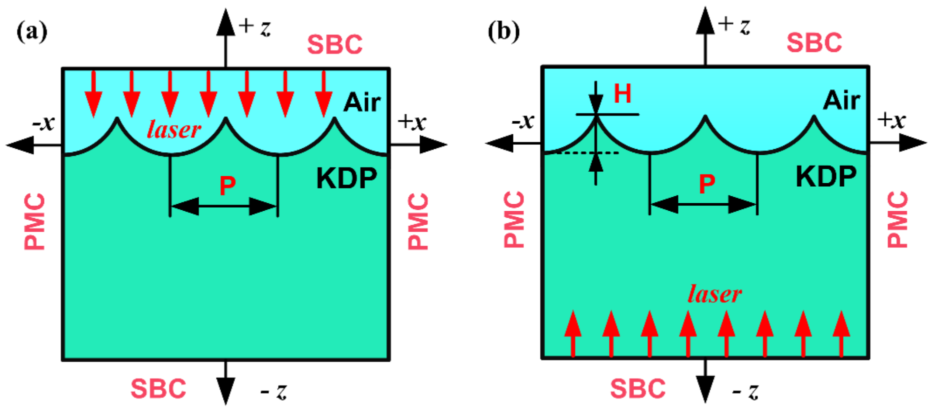

Fig. 4. The schematic of FEM model for simulating the EM fields caused by tool marks: (a) laser irradiates on KDP front-surface; (b) laser irradiates on KDP rear-surface.

Figure 4 presents the schematics of FEM model for simulating the electromagnetic field induced by front-and rear-surface tool marks, respectively. The cross-sections of repaired tool marks are in the x-z plane, and these tool marks are distributed along the x-axis while the feed direction of tool cutter is parallel to the y-axis. The period and residual height of tool marks are represented by P and H, respectively. To systematically investigate the influence of tool marks on its induced light field modulation inside KDP crystal, the periods of tool marks in the following simulation model were varied from 0.5 μm to 25 μm, and the corresponding residual heights changed from 50 nm to 250 nm in steps of 50 nm.

A time-harmonic plane electromagnetic wave with TE model, which has more serious modulation impact than that of TM mode [11], was chosen as the incident wave. The propagation direction of the 1ω (λ=1064 nm) plane wave is perpendicular to the KDP crystal. When this wave propagates along the +z-axis, it irradiates to the front surface. Otherwise, it irradiates to the rear surface. Meanwhile, the electric field intensity was normalized as 1V/m and the governing equation complies with Helmholtz equation [13]:

$$\nabla\times\left(\nabla\times \mathrm{E}\right)\text{-}\kappa^2\varepsilon_{\mathrm{r}}\mathrm{E}=0 \tag{1}$$

where ∇ is the differential operator, E, κ and ε_r denote the electric field intensity, wave number and relative dielectric constant, respectively.

To avoid the reflection of light at the boundary truncation, the scattering boundary conditions (SBC) is adopted in the wave incoming and outgoing surface. And the periodic boundary condition (PBC) is applied in the sides which parallel to ± Z axis. The mesh division in FEM models not only determines the quality of calculation results but also affects the efficiency of the simulation. Thus, all the below models employed two sizes of grids. Refined grids with a maximum size of 20 nm were used to mesh the regions around tool marks to guarantee the calculated accuracy, and slightly larger but no more than 50 nm grids were adopted to mesh the other areas in FEM model to improve the solution speed. Meanwhile, under the incident wave of 1064 nm, the relative dielectric constant ε_{r} is 1.49, the corresponding electric conductivity σ and relative magnetic permeability μ_{r} are 0 and 1.0, respectively.

With the aim to demonstrate the energy flow of electromagnetic waves inside KDP crystal, the Poynting vector (S) is introduced to describe the whole energy that passes through any unit area, perpendicular to the direction of wave propagation in any unit time. However, S is an instantaneous value that it is not easy to be detected. So the average of S is utilized to characterize the energy propagation of electromagnetic wave and this parameter is known as light intensity (I):

$$I = \frac{1}{\tau}\int_0^{\tau} Sdt = \left|\frac{1}{\tau}\int_0^{\tau} E \times Hdt\right| = \frac{1}{2}RE\left[E \times H^*\right] \tag{2}$$

where τ donates the time length of detection, * indicates the conjugate complex number, and the unit of light intensity (I) is W/m^2.

For time-harmonic plane electromagnetic wave, substitute $|E/H| = \sqrt{\mu/\varepsilon}$ to Eq. (2), and the light intensity can be expressed as:

$$I = \left|\frac{1}{T}\int_0^{T} E \times Hdt\right| = \frac{1}{2}RE\left[E \times H^*\right] = \frac{1}{2}\sqrt{\frac{\varepsilon}{\mu}}|E|^2 \tag{3}$$

It is clear to see that the light intensity is proportional to the square of electrical field ($|E^2|$). When the micro-milled surface is covered with tool marks, the light intensity inside KDP crystal will inevitably become unevenly distributed. Meanwhile, the light intensification has been widely accepted as the primary cause of the laser damage growth of KDP crystals in ICF facilities [34]. Therefore, on the basis of Eq. (3), the maximum relative light intensity modulation (I_{Rmax}) is introduced to describe the laser damage resistance of repaired KDP crystal with tool marks:

$$I_{\mathrm{Rmax}} = \frac{I_{\mathrm{max}}}{I_0} \tag{4}$$

where I_0 is the light intensity inside the flat KDP crystal with no tool marks, and I_{Rmax} is the largest light intensity inside micro-milled KDP crystal after the tool marks modulation. It is clear to see that the larger I_{Rmax} is, the more prone to laser damage the KDP optics are.

In addition, the light intensity I_0 was used to verify the feasibility and accuracy of the simulation model based on FEM method. It is found that the light intensity distributes evenly inside KDP crystal distributes evenly, and the numerical solution is I_0= 1.2759× 10^{-3}W/m^2. According to the theory of Fresnel reflections [38], the crystal internal light intensity is E=0.8032 V/m when it is under the normal irradiation of a TM mode wave which is normalized to 1V/m. As a result, the analytical solution of light intensity inside KDP crystal is derived from Eq. (3):

$$I = \frac{1}{2} RE\left[E \times H^{*}\right] = \frac{1}{2}\sqrt{\frac{\varepsilon}{\mu}}\left|E\right|^{2} = 1.2756 \times 10^{-3}\,\mathrm{W/m^{2}} \tag{5}$$

These results indicate a good agreement between the simulated and theoretically derived light intensity inside KDP crystal with an error of less than 0.02%. Therefore, the truncation constants and boundary conditions are reasonable, and this physical model built by FEM model is well validated.

4. Results and discussions

4.1 Light intensity modulation property of the period of tool marks

Figure 5 depicts the relative light intensity modulation curve with respect to tool mark periods on front- and rear-surface, respectively. One can see that the I_{Rmax} is very small when there are short-period tool marks (0.5 μm) on both surfaces of KDP crystal. And then, the modulation degrees rocket dramatically, amounting to the maximum at a tool mark period of 1 μm, followed by a remarkably drop despite slight fluctuations.

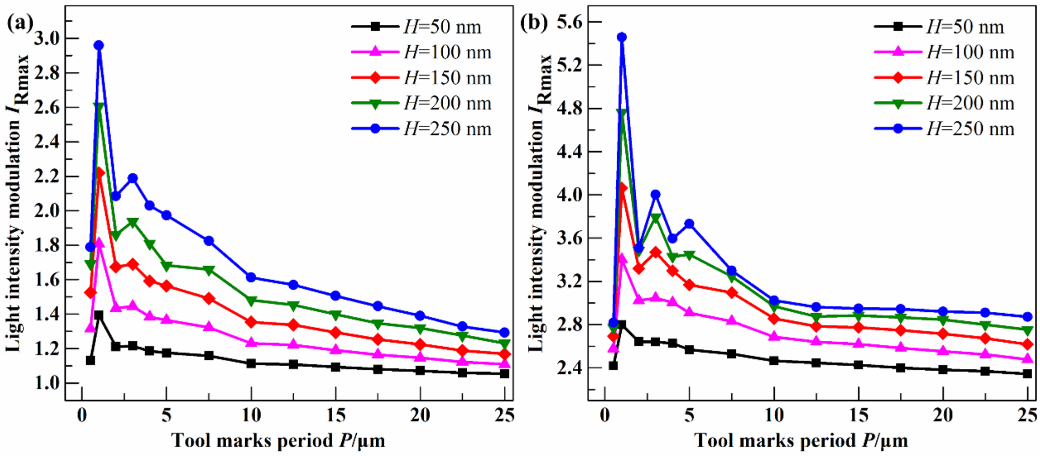

Fig. 5. The evolutions of I_{Rmax} induced by tool marks with respect to various periods (*P*): (a) tool marks on KDP front-surface; (b) tool marks on KDP rear-surface. The residual height (*H*) keeps constant as the tool mark period changes.

And from 10 μm onwards, the KDP crystal witnesses a moderately declining trend, and the relative light intensity modulations caused by tool marks with a period of 20 μm are approximately equal to that at the starting point (0.5 μm). It is noteworthy that the light intensity modulation I_{Rmax} induced by tool marks on rear-surface is greater than that on the front-surface from beginning to end, as shown in Fig. 5, although the I_{Rmax} with respect to tool marks period presents a consistent changing trend on both surfaces of KDP crystal.

Figure 6 exhibits the KDP crystal internal light intensity distribution caused by tool marks in case of P=0.5 μm and H=200 nm on its front-and rear-surface, respectively. As shown in Fig. 6(a), the ideal light field distorts noticeably after the modulation of tool marks on front-surface. The distorted regions with light intensity are distributed next to the machined surface, and they are perpendicular to the tool marks periodically. Because the dimensions of the tool marks are too small, the incident laser can only propagate through the KDP crystal surface in the form of evanescent waves and attenuates quickly along the light incident direction [33]. No obvious light intensification thus occurs in other regions inside the crystal. When it comes to the rear-surface tool marks, in addition to the above effects, the incident wave significantly interferes with the reflected wave, resulting in stationary waves, as shown in Fig. 6(b). This is the reason why the I_{Rmax} induced by the same tool marks on rear-surface is greater than that on front-surface. But looking at the overall variation trend of I_{Rmax}, there is no significant effect on the light intensity modulation induced by the small period tool marks (0.5 μm). It means that this size of tool marks for KDP crystal is conducive to resist the laser damage.

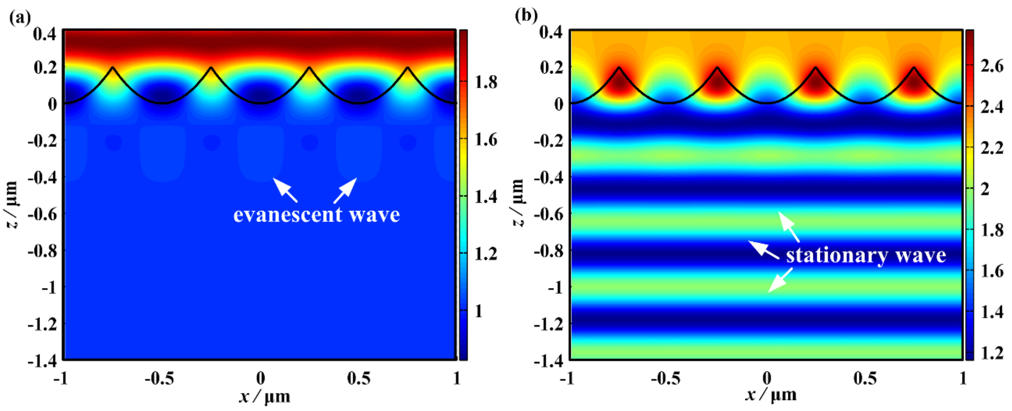

Fig. 6. The internal distributions of light intensity modulation induced by tool marks in case of P=0.5 μm and H=200 nm: (a) tool marks on KDP front-surface; (b) tool marks on KDP rear-surface.

However, considering the positional accuracy of machine tool and the ploughing effect in micro-machining area [19], it is very likely to cause the machined surface covered with heavy machining errors and enormous brittle micro-pits, which are all detrimental to the laser damage resistance of KDP optics. Furthermore, using this scale path interval (0.5 μm) are considerably time-consuming and inefficient to perform the actual repair work. Thus, the path interval with period of 0.5 μm should be selected cautiously when optimizing the machining parameters for repairing KDP optics.

As indicted in Fig. 5, the light intensifications become soaring exponentially, amounting to approximately 5.6, when the periods of tool marks are close to 1 μm. That is to say, in all probability, the KDP components repaired with this path interval are going to suffer from a new laser-induced damage again. The internal light intensity distributions at the presence of tool marks with parameters of P=1 μm and H=200 nm on both surfaces of KDP crystal are shown in Fig. 7. It is clear to say that the light intensity modulation regions periodically distribute not only parallel but also perpendicular to the direction of tool marks. The regions with intense light modulation (up to I_{Rmax}= 5.6) take place inside the KDP crystal with a period distribution, which is not conducive to resist the laser-induced damage for the repaired optics. The phenomenon is mainly attributed to the diffraction effect caused by tool marks [39]. The efficiency of ±1 order diffraction, which is the primary component in the diffraction effect in this situation, can normally reach the maximum and lead to a serious light intensification when the period of tool marks (1 μm) comes near the light wave length (1064 nm). This result is in good consistence with the diffraction property of micro-waves on fly-cut KDP surface [28, 33]. But it is important to highlight that the I_{Rmax} (3.0) caused by milled marks is nearly 1.5 times than that (2.1) caused by micro-waves with the same parameters on the front surface of KDP crystal, which means the tool marks have a greater adverse effect on the laser damage resistance of KDP optics than micro-waves. At the same time, the stationary waves are responsible for the higher I_{Rmax} on the KDP rear-surface just like the case in Fig. 6(b).

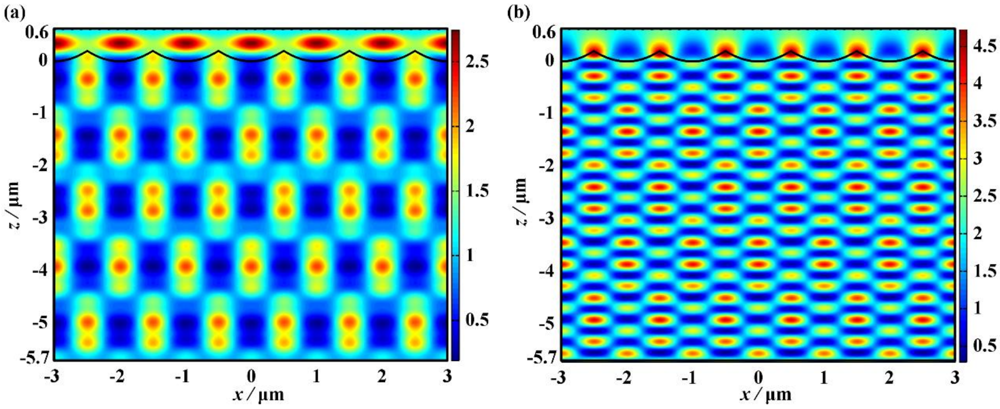

Fig. 7. The internal distributions of light intensity modulation induced by tool marks in case of *P*=1 μm and *H*=200 nm: (a) tool marks on KDP front-surface; (b) tool marks on KDP rear-surface.

From the wavelength sensitive period (1 μm) forwards, the relative light intensity modulation in Fig. 5 displays a sharply declining trend until 10 μm despite some slight fluctuations. The other orders (e.g. ±2, ±3, ±4) of the diffraction effect are regarded as the primary cause for these abrupt changes [33], and these diffractions orders would usually engage in modulating light intensification when tool marks period is around 2-5μm. Meanwhile, the diffraction efficiencies of these orders would be more significant when residual height is sufficiently high, causing that the I_{Rmax} in case of *H*=250 nm fluctuates more obvious than that in case of *H*=50 nm. Figure 8 presents the internal light intensity distribution induced by tool marks with parameters of *P*=0.5 μm and *H*=200 nm on both surfaces of KDP crystal, respectively. One can see that the diffraction effect plays a dominating role in modulating the light intensification. Meanwhile, it can be observed that the simulated patterns of light intensity modulation are similar with those exhibited in Fig. 7, which are distributed periodically both perpendicular and parallel to the tool marks. And it is clear to see that the period of light intensification parallel to tool marks is exactly equal to the tool marks period. But there are still two differences. The first one is that the maximal modulation degrees of light intensity in Fig. 8 are significantly lower than that associated with the presence of strong diffraction effect in Fig. 7. The other one is that the period of light intensification along the wave propagating direction becomes bigger, and a detailed discussion of this change will be provided below.

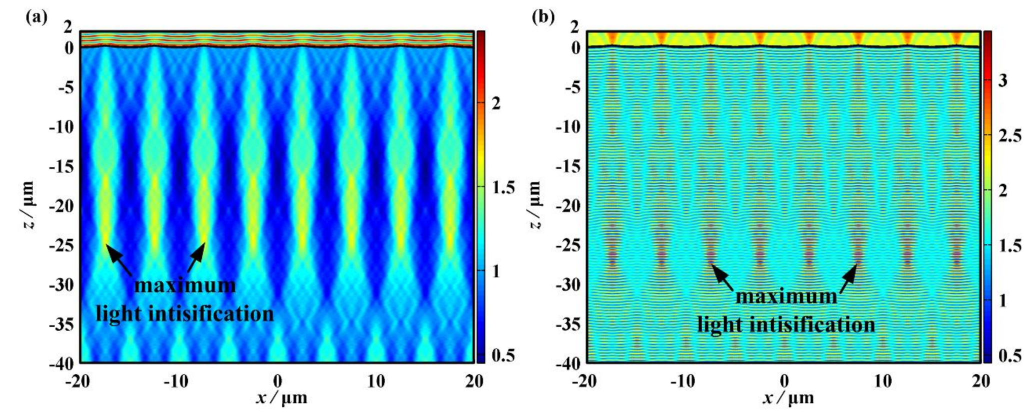

Fig. 8. The internal distributions of light intensity modulation induced by tool marks in case of P=5 μm and H=200 nm: (a) tool marks on KDP front-surface; (b) tool marks on KDP rear-surface.

As shown in Fig. 5, when the tool marks period is greater than 10 μm, the light intensity modulation decreases slightly with the increase of tool marks period. In particular, the I_{Rmax} caused by front-surface tool marks are basically close to that induced by tool marks with period of 1 μm, which is in form of evanescent wave. The internal light intensity distributions caused by tool marks with parameters of P=20 μm and H=200 nm on both sides of KDP crystal are presented in Fig. 9, respectively. It is found that the tool marks with a period of 20 μm generate a relative uniform light intensity distribution and a lower modulation degree with the largest I_{Rmax} of 1.3. The internal light intensification with respect to the front-surface tool marks originates from diffraction effect, which is caused by the summit of tool marks. The enhanced regions and weakened regions are both clearly visible, together forming diffraction ripples. This simulated pattern of diffraction ripples is very similar to the one caused by contamination particles, which is deduced through Fresnel diffraction theory [38]. When it comes to the rear-surface tool marks, the I_{Rmax} inside KDP is more than twice as large as that induced by front-surface marks. The higher light intensity modulation degree can be attributed to the stationary wave combined with diffraction effect.

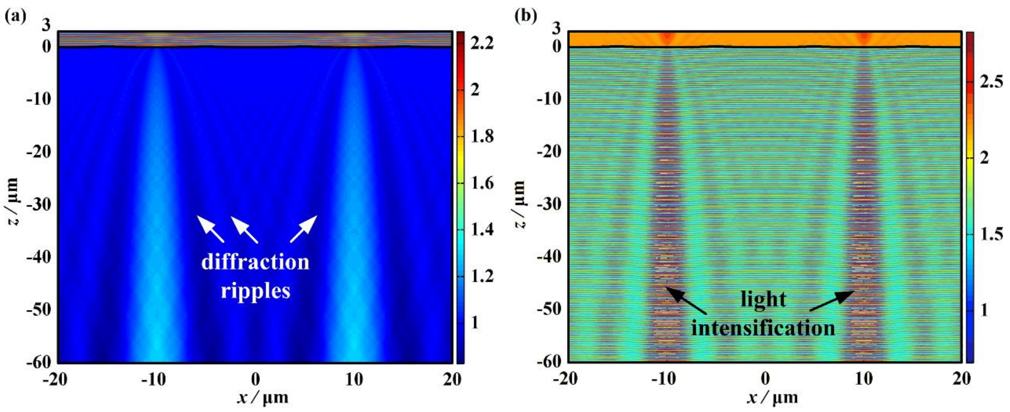

Fig. 9. The internal distributions of light intensity modulation induced by tool marks in case of P=20 μm and H=200 nm: (a) tool marks on KDP front-surface; (b) tool marks on KDP rear-surface.

Form the analysis above, it can be clearly seen that the light intensity modulation is periodically distributed along the direction of light propagation, and the relationship between its period P_z and the tool marks period P should be investigated. Because if the P_z is large, the distribution density of the maximal light intensification inside a fixed-thickness crystal will be small, indicating the milled crystal will be less susceptible to suffer from a new laser damage. To further investigate the relationship between P_z and P, a certain amount of sampling points was chosen based on the simulated result. The linear fitting result is presented in Fig. 10, in which the period P_z of light intensity is proportional to the square of tool marks period P. The expression can be described as follow:

$$P_z = \frac{2n_0}{\lambda} P^2 \tag{6}$$

It is found that the scale factor is twice the ratio of refractive index to wavelength. This may be due to that the adjacent tool marks will result in diffraction effect when irradiated by light wave, like the slits in double-slit diffraction event. Then, these diffraction waves will cause interference enhancement at some regions. Thus, the period of interference enhancement region is determined by the incident wavelength (λ), the refractive index of medium (n_0) and the distance of adjacent tool marks (P). Besides, this distributed pattern is very similar to the result caused by the interference grating as reported in Ref. [40].

If the tool marks period is set as 3 μm, by substituting it into Eq. (6), the light intensity period along z-axis is exactly to be 25 μm, which is in good agreement with simulated light intensity distribution caused by the tool marks with a period of 3 μm, as shown in Fig. 8(b).

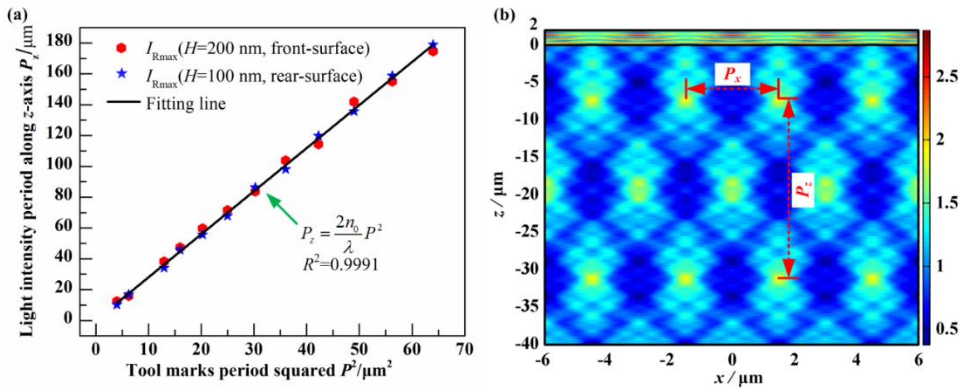

Fig. 10. (a)The fitting relation between tool marks period and the distribution period of light intensity along z-axis; (b) the internal distributions of light intensity modulation induced by tool marks on KDP front-surface in case of P=3 μm and H=200 nm.

As aforementioned, the light intensity period P_x along x-axis is equal to tool marks period. So on basis of P_z and P_x, it is very easy to predict the position where the I_{Rmax} appears inside the crystal, especially when the tool marks period and corresponding FEM model are too large to be solved by the limited computer memory. The locations of I_{Rmax} are normally the dangerous sites which are prone to be damaged by intense incident lasers.

Therefore, it is concluded that the possibility of a new laser-induced damage depends not only on its internal largest light intensity modulation I_{Rmax} caused by tool marks but also on the distribution density of I_{Rmax}. For a fixed-size KDP optic repaired by micro ball-end milling, if the maximum value and distribution density of the light intensity are both big, such as the case of light distribution caused by tool marks with a period of 1 μm presented by Fig. 7, the milled crystal optics possess high risk of laser-induced damage. From this perspective, the larger period tool marks are beneficial to improve the laser damage resistance and should be applied to the repair of damaged KDP optics. However, in practical micro-milling process, the relative large tool marks period usually results in the increase of machined surface roughness, which is specified to be less than 50 nm in

SG-III facilities. For instance, the surface roughness (Sa) machined with a path interval of 20 μm is 45 nm while the surface roughness machined with a path interval of 25 μm is 52.3 nm, which does not meet the requirement of SG-III facilities. Therefore, the tool paths corresponding to the tool marks with periods from 10 μm to 20 μm are preferred when optimizing the processing parameters in micro-milling repairing processes of KDP crystal.

4.2 Light intensity modulation property of the residual height of tool marks

To have a better understanding on the effect of tool marks residual heights on the light intensity modulation, the periods of tool marks used in this study were set as 1 μm, 5 μm, 10 μm, 20 μm, 25 μm, respectively, while the residual heights of tool marks change from 50 nm to 250 nm. Figure 11 shows the simulation results of internal light intensification caused by tool marks with respect to heights on both surfaces of KDP crystal. For various periods, as the residual height of tool marks increases, the maximum light intensity modulation inside the crystal shows an overall upward trend, albeit with different rake ratio. Taking the period of 1 μm for instance, the light intensity modulation becomes higher as the residual height increases no matter whether the tool marks are on front-surface or rear-surface, as shown in Fig. 11. The internal light intensity distributions caused by tool marks with parameters of P=1 μm and H=50 nm on both surfaces of KDP crystal are presented in Fig. 12, respectively. It is found that the light intensity distributes more uniformly than that observed from Fig. 7. This is because the light field would be distorted due to the diffraction caused by tool marks, and the higher the tool marks, the more severe the light field distorted. Another distinction is that the increment of I_{Rmax} on rear-surface from 50 nm to 200 nm is about 2.0, while the corresponding increment of I_{Rmax} on front-surface is only 1.1. As aforementioned, this observation is attributed to the effect of stationary wave.

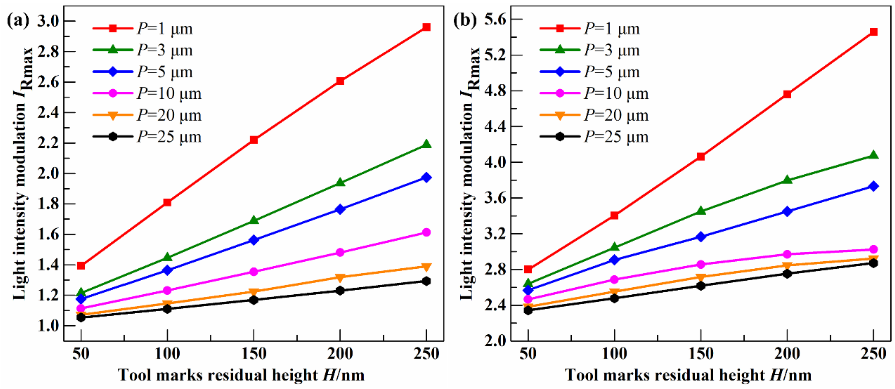

Fig. 11. The evolutions of I_{Rmax} induced by tool marks with respect to residual height (H): (a) tool marks on KDP front surface; (b) tool marks on KDP rear surface. The tool marks period (P) keeps constant as the residual height changes.

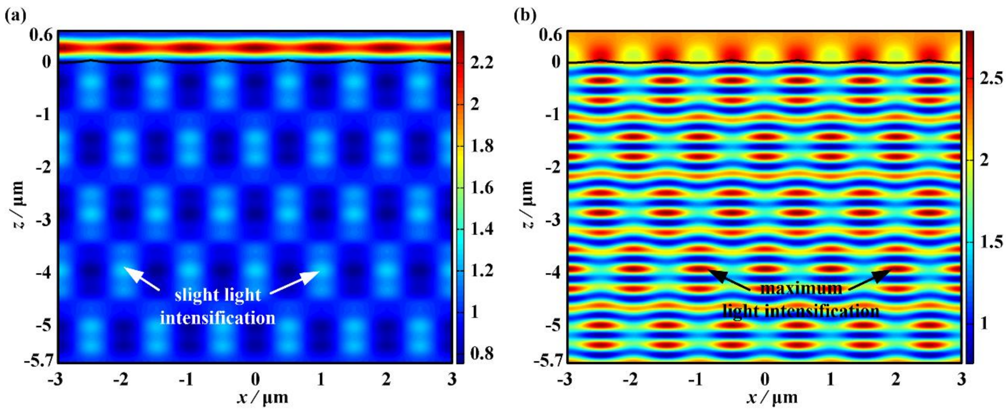

Fig. 12. The internal distributions of light intensity modulation induced by tool marks in case of P=1 μm and H=50 nm: (a) tool marks on KDP front surface; (b) tool marks on KDP rear surface.

Figure 13 presents the internal light intensity at the presence of tool marks with parameters of P=20 μm and H=50 nm on both surfaces of KDP crystal. Compared with the light field shown in Figs. 9(a) and 9(b), the distribution patterns of light intensity at 50 nm are consistent with that at 200 nm in spite of the tool marks on the front- or rear-surface. Although the light intensity ascends with the increase of residual height, the actual change of I_{Rmax} is not significant. This is because the efficiency of diffraction effect declines noticeably when the tool marks period is far away from the wavelength [33]. At the same time, for tool marks with period of 10 μm and 20 μm, no matter whether they are on the front- or rear-surface, the induced I_{Rmax} with respect to all residual heights is almost at a comparatively low level, which means the residual height of tool marks has a very gentle modulation to the light intensity. The discovery is in good agreement with the results shown in Fig. 5.

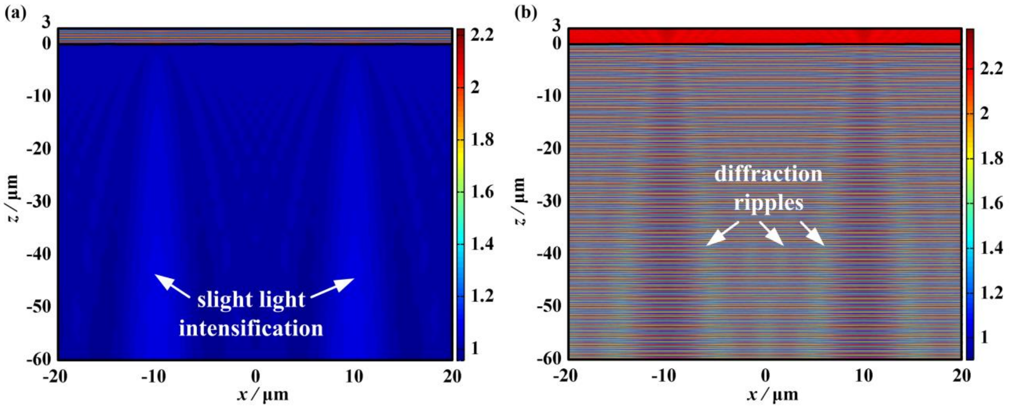

Fig. 13. The internal distributions of light intensity modulation induced by tool marks in case of P=20 μm and H=50 nm: (a) tool marks on KDP front-surface; (b) tool marks on KDP rear-surface.

In addition, on the basis of the above discussion, it is concluded that the tool marks generated on KDP crystal in the micro ball-end milling process can cause severe internal light intensification, and thus have an adverse effect on the laser-induced damage resistance of repaired KDP optics. The periods of tool marks mainly determine the distribution patterns as well as the densities of light intensity, which is normally parallel and perpendicular to tool marks, while the residual height of tool marks only plays a slight role in determining the maximum light intensity (I_{Rmax}). The distribution density and maximum I_{Rmax} jointly determine the light intensification inside the repaired optics. Once the induced light intensity becomes high enough, the photo-ionization and impact ionization processes of KDP material would take place [41]. As a result, laser-induced damage may occur catastrophically under the high-power laser irradiations. However, as an inherent feature of ball-end milling, the tool marks are inevitably generated on the machined surface [27]. The only thing that can be done is to actively control it and choose relatively reasonable machining parameters. According to the simulation results, tool marks with relatively large period and small residual height are beneficial to reduce the light intensity modulation inside the crystal and correspondingly enhance the ability to resist to laser damage. Considering the actual machining efficiency and surface quality, the path interval from 10 μm to 20 μm and relative small residual height of tool marks should be preferred in the practical repairing process of KDP optics in ICF facilities.

4.3 Test of optical transmittance and laser damage of micro-milled KDP surfaces

Figure 14 exhibits the measured optical performance of the micro-milled KDP front surfaces with various period tool marks, as well as a fly-cut KDP surface (no tool marks). Dual coordinates are adopted to demonstrate the results, where the abscissa is the typical periods of tool marks, and the left ordinate donates the optical transmittance while the right ordinate is the laser-induced damage thresholds. The error bars indicate the standard deviation of the measured results of 10 test sites, and these errors mainly resulted from the uncertainty of the initiation of laser-induced damage events and the intrinsic errors existing in the measuring systems [10].

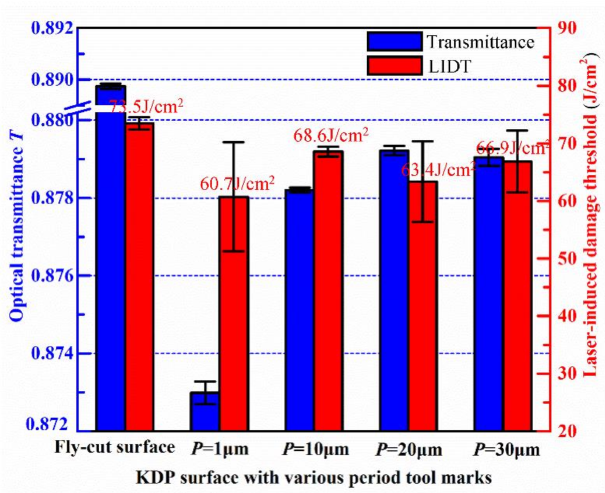

Fig. 14. The measured optical transmittance and laser-induced damage threshold (LIDT) of the micro-milled KDP front surfaces with tool marks in various period (P) and one fly-cut KDP surface. The error bars indicate the standard deviation of the measured results of 10 test sites.

As illustrated in Fig. 14, the micro-milled surfaces witness an obvious rise in the optical transmittance at first as the tool marks period increases, followed by a plateau with a slight fluctuation. It is noteworthy that there is no obvious difference even the error bars were taken into account. When it comes to the tool marks with period of 1 μm, the sample surface possesses the lowest transmittance (T=87.3%), which coincides well with the observation from Fig. 5 that tool marks with this scale (P=1 μm) could easily induce the strongest light intensity modulation inside KDP crystal and consequently cause enormous light loss. It could also be proved by the transmittance curves under a broad range of wavelengths, as shown in Fig. 15. One can see that, the transmittance for 1 μm samples is definitely lower that for samples with other tool mark periods. As for other three kinds of tool marks, the transmittance amounts to 87.9% at the period of 20 μm, which means the micro-milled surface machined by this path interval can have a great positive effect on the transmittance of repaired KDP optics.

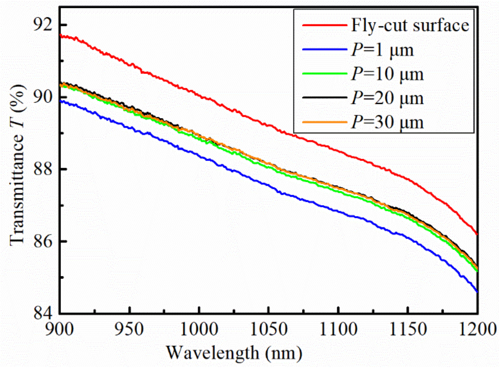

Fig. 15. The transmittances of various machined surface in a broad wavelength range.

Furthermore, as shown in Fig. 14, the tested LIDTs also present the same trend with transmittance. It can be seen that the micro-milled KDP surface with tool marks (P=1 μm) has the minimum LIDT (60.7 J/cm^2) among all the measured objects, while the LIDT of initial fly-cut KDP surface is up to 73.5 J/cm^2. This result further proves that tool marks with 1 μm period can cause severe light intensity modulation when irradiated by high power density laser and give rise to new damage, thereby weaken the repair effectiveness of KDP optics. Therefore, the path interval (P=1 μm) should not be adopted in the practical repairing work of KDP optics as well as the future routine operation of ICF facilities. While for other three kinds of tool marks, the LIDTs are high and the maximum LIDT can reach up to 68.6 J/cm^2 at 10 μm, which is pretty close to that of fly-cut surface.

Figure 16 displays the typical laser damage morphologies of the measured surfaces with respect to the periods of 1 μm and 20 μm. One can see the damage cracks normally take place in the vicinity of the tool marks, indicating that tool marks on the micro-milled

KDP surfaces are the vulnerable features of being damaged. As shown in Fig. 7, the calculated light intensification is strengthened up to 5.6 times inside KDP optics surface with tool marks period of 1 μm. These hot spots of light intensification can be focused to several micrometers beneath the surface. With increase of laser shots, these hot spots would accumulate more energy and undergo severe thermal absorbing [20]. Once the temperature near these spots exceeds the critical value of damage initiation, the laser-induced damage would occur catastrophically on the optics surface in forms of cracks [37, 41], as shown in Fig. 16(a). In addition, a black ring is generated on the machined surface with tool marks period of 1 μm due to the laser cleaning effect [42, 43]. When adopting a very small path interval, some generated chips would adhere to the machined surface and would be melted and vaporized firstly once machined samples are irradiated by a high-power laser. This phenomenon is very similar to the visible rings generated on fused silica surfaces under CO_2 laser irradiation. The polishing swirls and scratches on silica surface are very easy to be melted and vaporized due to the laser cleaning effect, introducing black rings on the fused silica surface [42]. While for the micro-milled surface with tool marks period of 20 μm, the damage morphology is not as clear as that in case of 1 μm period. This is because of the hot spots of light intensification located far beneath the micro-milled surface. According to Eq. (6) and the fitting curve shown in Fig. 10 (a), the distance between these hot spots and machined surface is more than one thousand micrometers. It means that once the laser-induced damage takes place, it would also be inside the optic and far away from the micro-milled surface. Therefore, these damage morphologies in case of tool marks period of 20 μm could not be clearly observed by optical microscope.

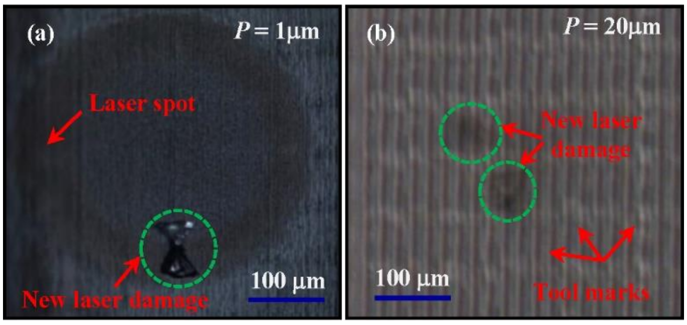

Fig. 16. Morphologies of the laser damage on the micro-milled KDP surfaces with tool mark periods of 1μm (a) and 20μm (b). The applied laser fluences are 62.8J/cm^2 and 69.1J/cm^2, respectively.

5. Conclusion

In this work, the influence of the period and residual height of tool marks generated in micro ball-end milling process on the light intensifications inside KDP optics is theoretically analyzed and the experiment verification is performed. It was found that the period of tool marks exerts a dominant effect on the induced I_{Rmax}, when compared with its residual height. Tool marks with a period of 1 μm could cause up to 5.6 times I_{Rmax}, meaning that the corresponding milled surfaces are more susceptible to be damaged. The regions with induced light intensification distribute periodically inside KDP optics. The period of light intensification is strongly associated with the period of tool marks. The greater the period of tool marks, the smaller the density of light intensification occurs, indicating the less possibility of laser damage. Nearly twice higher I_{Rmax} is caused by the rear-surface tool marks than that induced by the front-surface ones due to interference effect. This is the reason why KDP rear-surface is easier to be damaged than its front-surface. The transmittance and laser damage tests on micro-milled KDP surfaces jointly verified that the tool marks with 1 μm period have devastating impact on the laser damage resistance of repaired KDP optics, while the milled surfaces covering tool marks with periods from 10 μm to 20 μm possess similar LIDTs and transmittance capacities comparable to those of fly-cut surfaces. Thus, the machining parameters corresponding to tool marks (periods in 10~20 μm) are recommended in the practical micro-milling repairing of full-aperture KDP optics.

Acknowledgments

This work is financially supported by the National Natural Science Foundation of China (No. 51775147, No. 51705105), Science Challenge Project (No. TZ2016006-0503-01), China Postdoctoral Science Foundation funded project (No. 2017M621260), Heilongjiang Postdoctoral Fund (No. LBH-Z17090) and Self-Planned Task (No. SKLRS201718A) of State Key Laboratory of Robotics and System (HIT). The first author also highly appreciates the support from China Scholarship Council.

Competing Interests

The authors declare that they have no competing interests.

Reference

[1] E.I. Moses, W.R. Meier, Preparing for ignition experiments on the National Ignition Facility, Fusion Eng. Des. 83 (2008) 997–1000. https://doi.org/10.1016/j.fusengdes.2008.05.043.

[2] R.F. Su, H.T. Liu, Y.Ch. Liang, F.L. Yu, Residual thermal stress of a mounted KDP crystal after cooling and its effects on second harmonic generation of a high-average-power laser, Opt. Laser Technol. 87 (2017) 43-50. http://dx.doi.org/10.1016/j.optlastec.2016.07.018.

[3] C.J. Stolz, The national ignition facility: the path to a carbon-free energy future, Phil. Trans. R Soc. A 370 (2012) :4115–4129. https://doi.org/10.1098/rsta.2011.0260.

[4] A. Casnera, T. Caillauda, S. Darbona, A. Duvala, R. Wrobela, J.L. Miquela, LMJ/PETAL laser facility: Overview and opportunities for laboratory astrophysics, High Energy Density Phys. 17 (2015) 2–11. https://doi.org/10.1016/j.hedp.2014.11.009.

[5] Z. Zhang, H. Wang, X.S. Quan, G.Q. Pei, M.J.Y. Tian, T.Y. Liu, K. Long, P.D. Li, Y.M. Rong, Optomechanical analysis and performance optimization of large-aperture KDP frequency converter, Opt. Laser Technol. 109 (2019) :633–642. https://doi.org/10.1016/j.optlastec.2018.08.053.

[6] S.F. Wang, J. Wang, Q. Xu, X.Y. Lei, Z.C. Liu, J.F. Zhang, Influences of surface defects on the laser induced damage performances of KDP crystal, Appl. Optics 57 (2018) 2638–2646. https://doi.org/10.1364/AO.57.002638.

[7] M.L. Spaeth, P.J. Wegner, T.I. Suratwala, M.C. Nostrand, Optics recycle loop strategy for NIF operations above UV laser–induced damage threshold, Fus. Sci. Technol. 69 (2016) 265–294. https://doi.org/10.13182/FST15-119.

[8] W.L. Hrubesh, R.M. Brusasco, W. Grundler, et al, Methods for mitigating growth of laser-initiated surface damage on DKDP optics at 351nm, Proc SPIE 4932 (2003) 180–191. https://doi.org/10.1117/12.472047.

[9] Y.B. Zheng, R. Sh. Ba, X.D. Zhou, L. Ding, J. Li, J. Yuan, H.L. Xu, J. Na, B. Chen, W.G. Zheng, Characteristics of precursors responsible for bulk damage initiation in doubler KDP crystal at different wavelengths, Opt. Laser Technol. 96 (2017) 196-201. https://doi.org/10.1016/j.optlastec.2017.05.034.

[10] P. Gereghty, W. Carr, V. Draggoo, R. Hackel, C. Mailhiot, M. Norton, Surface damage growth mitigation on KDP/DKDP optics using single-crystal diamond micro-machining ball end mill contouring, Proc SPIE 6403 (2007) 64030Q. https://doi.org/10.1117/12.696076.

[11] J. Cheng, M.J. Chen, W. Liao, J.H. Wang, Y. Xiao, M.Q. Li, Fabrication of spherical mitigation pit on KH_2PO_4 crystal by micro-milling and modeling of its induced light intensification, Opt. Express 21 (2013) 16799–16813. https://doi.org/10.1364/OE.21.016799.

[12] F. Guillet, B. Bertussi, L. Lamaignere, X. Leborgne, B. Minot, Prelimininary results on mitigation of KDP surface damage using ball dimpling method, Proc SPIE 6720 (2007) 672008. https://doi.org/10.1117/12.752822.

[13] H. Yang, J. Cheng, M.J. Chen, J. Wang, Z.C. Liu, Q. Liu, Optimization of morphological parameters for mitigation pits on rear KDP surface: experiments and numerical modeling, Opt. Express 25 (2017) 18332–18345. https://doi.org/10.1364/OE.25.018332.

[14] D.X. Zhu, Y.G. Li, Q.H. Zhang, J. Wang, Q. Xu, Laser induced damage due to scratches in the surface of nonlinear optical crystals KH_2PO_4 (KDP), J. EUR. OPT. SOC-RAPID. (2017) 13-33. https://doi.org/10.1186/s41476-017-0062-8.
[15] Q. Liu, J. Cheng, Y. Xiao, H. Yang, M.J. Chen, Influence of milling modes on surface integrity of KDP crystal processed by micro ball-end milling, Proc CIRP 71 (2018) 260–266. https://doi.org/10.1016/j.procir.2018.05.060.
[16] S.F. Wang, C.H. An, F.H. Zhang, Z.F. Zhang, An experimental and theoretical investigation on the brittle ductile transition and cutting force anisotropy in cutting KDP crystal. Int. J. Mach. Tools Manuf. 106 (2016) 98-108. https://doi.org/10.1016/j.ijmachtools.2016.04.009.
[17] Y. Xiao, M.J. Chen, Y.T. Yang, J. Cheng, Research on the critical condition of brittle-ductile transition about micro-milling of KDP crystal and experimental verification. Int. J. Precis. Eng. Man. 16 (2015) 351–359. https://doi.org/10.1007/s12541-015-0046-9.
[18] N. Chen, M.J. Chen, Y.Q. Guo, X.B. Wang, Effect of cutting parameters on surface quality in ductile cutting of KDP crystal using self-developed micro PCD ball end mill. Int. J. Adv. Manuf. Tech. 78 (2015) 221–229. https://doi.org/10.1007/s00170-014-6623-8.
[19] Q. Liu, J. Cheng, Y. Xiao, M.J. Chen, H. Yang, J.H. Wang, Effect of tool inclination on surface quality of KDP crystal processed by micro ball-end milling, Int. J. Adv. Manuf. Technol. 99 (2018) 2777-2788. https://doi.org/10.1007/s00170-018-2622-5.
[20] J. Cheng, M.J. Chen, W. Liao, H.J. Wang, J.H. Wang, Y. Xiao, M.Q. Li, Influence of surface cracks on laser-induced damage resistance of brittle KH_2PO_4 crystal, Opt. Express 24 (2014) 28740–28755. https://doi.org/10.1364/OE.22.028740.
[21] Z.R. Liao, D. Axinte, D. Gao, A novel cutting tool design to avoid surface damage in bone machining, Int. J. Mach. Tools Manuf. 106 (2017) 52-59. https://doi.org/10.1016/j.ijmachtools.2017.01.003
[22] N. Chen, M.J. C.Y. Wu, X.D. Pei, Cutting surface quality analysis in micro ball end-milling of KDP crystal considering size effect and minimum undeformed chip thickness, Preci. Eng. 50 (2017) 410–420. https://doi.org/10.1016/j.precisioneng.2017.06.015.
[23] Y.T. Yu, P. Wang, Y.C. Zhu, J.S. Diao, Broadband metallic planar microlenses in an array: the focusing coupling effect, Nanoscale Res. Lett.11 (2016) 109. https://doi.org/10.1115/1.4001037.
[24] Z.W. Zhu, S. To, S.J. Zhang, Active control of residual tool marks for freeform optics functionalization by novel biaxial servo assisted fly cutting, Appl. Opt. 54 (2015)7656-7662. https://doi.org/10.1364/AO.54.007656.
[25] L. Li, S.A. Collins, A.Y. Yi, Optical Effects of Surface Finish by Ultraprecision Single Point Diamond Machining, J. Manuf. Sci E-T ASME 132 (2010) 021002. https://doi.org/10.1115/1.4001037.
[26] Z. W. Zhu, X.Q. Zhou, D. Luo, Development of pseudo-random diamond turning method for fabricating freeform optics with scattering homogenization, Opt. Express 21 (2013) 28469–28482. https://doi.org/10.1364/OE.21.028469.
[27] J.H. Chen, K.Y. Huang, M.S. Chen, A study of the surface scallop generating mechanism in the ball-end milling process, Int. J. Mach. Tool Manu. 45 (2005) 1077–1084. https://doi.org/10.1016/j.ijmachtools.2004.11.019.
[28] M.J. Chen, M.Q. Li, W. Jiang, Q. Xu, Influence of period and amplitude of micro-waveness on crystal's laser damage threshold, J. Appl. Phys. 108 (2010) 043109. https://doi.org/10.1063/1.3462430.

[29] M.Q. Li, Study on influence of KDP crystal ultra-precision fly-cutting micro/nano-topography on its laser induced damage threshold. Harbin: Harbin Institute of Technology 2013, 41-47.
[30] M.Q. Li, M.J. Chen, C.H. An, L. Zhou, J. Cheng, W. Jiang, Mechanism of micro-waviness induced KH2PO4 crystal laser damage and the corresponding vibration source, Chinese Phys. B 21 (2012) 050301. https://iopscience.iop.org/article/10.1088/1674-1056/21/5/050301.
[31] M.J. Chen, J. Chen, X.D. Yuan, Role of tool marks inside spherical mitigation pit fabricated by micro-milling on repairing quality of damaged KH_2PO_4 crystal, Sci. Rep. 5 (2015) 14422. doi: 10.1038/srep14422.
[32] M.J. Chen, Q.L. Pang, X.Y. Liu, Finite element analysis on influence of micro-nano machined surface impurity on optical performance of crystal, High Power Laser and Particle Beams, 20 (2008) 1182-1186.
[33] M.J. Chen, W. Jiang, M.Q. Li, K.N. Chen, Study of the near-field modulation property of micro-waveness on a KH_2PO_4 crystal surface, Chinese Phys. B 19 (2010) 064203. https://doi.org/10.1088/1674-1056/19/6/064203.
[34] N.L. Boling, G. Dubé, M.D. Crisp, Laser induced surface damage. Appl. Optics 12(1973) 650–660. https://doi.org/10.1364/AO.12.000650.
[35] Y. Xiao, M.J. Chen, X. Chu, T.L. Tian, Research on accuracy analysis and performance verification test of micro-precise five-axis machine tool, Int. J. Adv. Manuf. Technol. 67 (2013) 387–395. https://doi.org/10.1007/s00170-012-4492-6.
[36] J. Cheng, Y. Hao, Q. Liu, M.J. Chen, W.J. Ma, J.B. Tan, Z.C. Liu, Development of optimal mitigation contours and their machining flow by micro-milling to improve the laser damage resistance of KDP crystal, Proc. SPIE 10447L (2017) https://doi.org/10.1117/12.2280519.
[37] Z.C. Liu, F. Geng, Y.G. Li, J. Cheng, H. Yang, Y. Zheng, J. Wang, Q. Xu, Study of morphological feature and mechanism of potassium dihydrogen phosphate surface damage under a 351 nm nanosecond laser, Appl. Opt. 57 (2018) 10334-10341. https://doi.org/10.1364/AO.57.010334.
[38] N.L. Boling, G. Dubé, M.D. Crisp, Morphological asymmetry in laser damage of transparent dielectric surfaces, Appl. Phys. Lett. 21 (1972) 487–489. https://doi.org/10.1063/1.1654229.
[39] C.L. He, W.J. Zong, Diffraction effect and its elimination method for diamond-turned optics, Opt. Express 27 (2019) 1326-1344. https://doi.org/10.1364/OE.27.001326.
[40] R.V. Litvinov, Photorefractive response of a cubic gyrotropic crystal with applied square-wave electric field on the interference grating with large contrast, Proc. SPIE 4751 (2001) 270–281. https://doi.org/10.1117/12.475920.
[41] J. Cheng, M.J. Chen, K. Kafka, D. Austin, J.H. Wang, Y. Xiao, E. Chowdhury, Determination of ultra-short laser induced damage threshold of KH_2PO_4 crystal: Numerical calculation and experimental verification, AIP Adv. 6 (2016) 035221. https://doi.org/10.1063/1.4945415.
[42] E. Mendez, H.J. Baker. K.M. Nowak, Highly localised CO2 laser cleaning and damage repair of silica optical surfaces, Proc. SPIE 5467 (2004). https://doi.org/10.1117/12.585293.
[43] S. Papernov, A.W. Schmid, Laser-induced surface damage of optical materials: Absorption sources, initiation, growth, and mitigation, Proc. SPIE 7132 (2008). https://doi.org/10.1117/12.804499.

Figures Legend

Fig. 1. Pictures of the machining set-up used in this work. (a) The micro-milling five-axis machine tool. (b) The micro ball-end milling cutter. (c) Schematic of the formation of tool marks.

Fig. 2. Morphology of tool marks measured by white light interferometer. The residual height and path interval of tool marks are about 199 nm and 20 μm, respectively.

Fig. 3. Schematic of the laser system designed to test the LIDTs of micro-milled KDP surfaces.

Fig. 4. The schematic of FEM model for simulating the EM fields caused by tool marks: (a) laser irradiates on KDP front-surface; (b) laser irradiates on KDP rear-surface.

Fig. 5. The evolutions of I_{Rmax} induced by tool marks with respect to various periods (*P)*: (a) tool marks on KDP front-surface; (b) tool marks on KDP rear-surface. The residual height (*H*) keeps constant as the tool mark period changes.

Fig. 6. The internal distributions of light intensity modulation induced by tool marks in case of *P*=0.5 μm and *H*=200 nm: (a) tool marks on KDP front-surface; (b) tool marks on KDP rear-surface.

Fig. 7. The internal distributions of light intensity modulation induced by tool marks in case of *P*=1 μm and *H*=200 nm: (a) tool marks on KDP front-surface; (b) tool marks on KDP rear-surface.

Fig. 8. The internal distributions of light intensity modulation induced by tool marks in case of *P*=5 μm and *H*=200 nm: (a) tool marks on KDP front-surface; (b) tool marks on KDP rear-surface.

Fig. 9. The internal distributions of light intensity modulation induced by tool marks in case of *P*=20 μm and *H*=200 nm: (a) tool marks on KDP front-surface; (b) tool marks on KDP rear-surface.

Fig. 10. (a)The fitting relation between tool marks period and the distribution period of light intensity along z-axis; (b) the internal distributions of light intensity modulation induced by tool marks on KDP front-surface in case of P=3 μm and H=200 nm.

Fig. 11. The evolutions of I_{Rmax} induced by tool marks with respect to residual height (*H*): (a) tool marks on KDP front surface; (b) tool marks on KDP rear surface. The tool marks period (*P*) keeps constant as the residual height changes.

Fig. 12. The internal distributions of light intensity modulation induced by tool marks in case of *P*=1 μm and *H*=50 nm: (a) tool marks on KDP front surface; (b) tool marks on KDP rear surface.

Fig. 13. The internal distributions of light intensity modulation induced by tool marks in case of *P*=20 μm and *H*=50 nm: (a) tool marks on KDP front-surface; (b) tool marks on KDP rear-surface.

Fig. 14. The measured optical transmittance and laser-induced damage threshold (LIDT) of the micro-milled KDP surfaces with tool marks in various period (P) and one fly-cut KDP surface. The error bars are the standard deviation of the measured results of 10 test sites.

Fig. 15. Morphologies of the laser damage on the micro-milled KDP surfaces with tool mark periods of 1μm (a) and 20μm (b). The applied laser fluences are 62.8J/cm^2 and 69.1J/cm^2, respectively.